Influence of the Initiator System on the Spatial Inhomogeneity in Acrylamide-Based Hydrogels

Nermin Orakdogen, Oguz Okay

Istanbul Technical University, Department of Chemistry, 34469 Maslak, Istanbul, Turkey

Received 26 January 2006; accepted 19 June 2006
DOI 10.1002/app.24977
Published online in Wiley InterScience (www.interscience.wiley.com).

ABSTRACT: The effect of the initiator system used in the gel preparation on the spatial inhomogeneity in poly(acrylamide) (PAAm) and poly(*N*,*N*-dimethylacrylamide) (PDMA) hydrogels was investigated by static light scattering and elasticity measurements. The hydrogels were prepared by free-radical crosslinking copolymerization of the monomers acrylamide (AAm) or *N*,*N*-dimethylacrylamide (DMA) with *N*,*N*′-methylenebisacrylamide as a crosslinker. Two different redox-initiator systems, ammonium persulfate (APS)–*N*,*N*,*N*′,*N*′-tetramethylethylenediamine (TEMED) and APS–sodium metabisulfite (SPS), were used to initiate the gelation reactions. Compared to the APS–TEMED redox pair, no significant scattered light intensity rise was observed during the crosslinking polymerization reactions initiated by the APS–SPS system. It was found that both PAAm and PDMA gels are much more homogeneous when the APS–SPS redox pair was used as the initiator. The results are explained by the formation of shorter primary chains as well as the delay of the gel point in APS–SPS initiated gel formation reactions. © 2006 Wiley Periodicals, Inc. J Appl Polym Sci 103: 3228–3237, 2007

Key words: hydrogels; redox initiator; inhomogeneity; static light scattering; gelation

INTRODUCTION

Free-radical crosslinking copolymerization (FCC) of acrylamide (AAm)-based monomers has been widely used to synthesize polymer hydrogels. As is well known, gelation during FCC occurs nonrandomly due to the existence of various nonidealities such as the conversion and structure-dependent reactivities of the functional groups, cyclization, and multiple crosslinking reactions.[1,2] These nonidealities during gelation necessarily result in the formation of polymer gels with a large number of network defects, affecting their physical properties such as swelling, elasticity, transparency, and permeability. One of the network defects is the inhomogeneous distribution of the crosslink points along the gel sample, which is known as the spatial gel inhomogeneity.[3,4] Since the gel inhomogeneity is closely connected to the spatial concentration fluctuations, scattering methods have been employed to investigate the spatial inhomogeneities.[5–10] The gel inhomogeneity can be manifested by comparing the scattering intensities from the gel and from a semidilute solution of the same polymer at the same concentration. The scattering intensity from gels is always larger than that from the polymer solution. The excess scattering over the scattering from polymer solution is related to the degree of the inhomogeneities in gels.

Spatial gel inhomogeneity in the final materials is undesirable for applications because structural inhomogeneity results in a dramatic reduction in the strength of the crosslinked materials. Although the inhomogeneity control in gels is quite sophisticated, the ionization of polymer gels is one of the methods used to suppress the inhomogeneities.[3,4,11,12] Moreover, at a given polymer concentration, that is, at a fixed swelling degree of gels at the state of the inhomogeneity measurement, reducing the crosslinker concentration also reduces the degree of spatial gel inhomogeneity.[13] On the other hand, if a gel sample swells beyond its dilution degree after its preparation, the spatial inhomogeneity increases.[14] Recently, we have shown that the spatial gel inhomogeneity can be controlled by varying the gel point with respect to the critical overlap concentration during the gel preparation stage.[15]

The effect of the initiator system used in the gelation reactions on the gel inhomogeneity has not been reported before. Here, we investigated the formation processes of poly(acrylamide) (PAAm) and poly(*N*,*N*-dimethylacrylamide) (PDMA) gels by time-resolved light scattering. To convert the independent variable reaction time to the monomer conversion, a dilatometric technique was also used to monitor the polymerization reactions. We used two different redox-initiator systems to initiate the gelation reactions of AAm

Correspondence to: O. Okay (okayo@itu.edu.tr).
Contract grant sponsor: Scientific and Technical Research Council of Turkey (TUBITAK); contract grant number: TBAG-105T246.

Journal of Applied Polymer Science, Vol. 103, 3228–3237 (2007)

as well as *N,N*-dimethylacrylamide (DMA) monomers in the presence of *N,N′*-methylenebisacrylamide (BAAm) as a crosslinker. The first initiator system, ammonium persulfate (APS)–*N,N,N′,N′*-tetramethylethylenediamine (TEMED) redox pair, is widely used in the gel formation reactions. The free radicals generated on TEMED molecules initiate the polymerization reaction and the rate is about three times that in the absence of a TEMED accelerator.[16] The second initiator system we used in our experiments is the APS–sodium metabisulfite (SPS) redox pair. Although the mechanism has not yet been established, free-radical generation by the latter redox pair occurs using metabisulfite as well as bisulfite anions.[17,18] Further, in the presence of oxygen the bisulfite ion can also couple with oxygen to form a redox pair to generate free radicals, initiating the polymerization.[19] Therefore, free-radical polymerization initiated by the APS–SPS redox pair in the presence of oxygen consists of several competitive initiation steps. Indeed, our preliminary experiments showed that the polymerization rates of both AAm and DMA monomers in the presence of APS–SPS and air are initially slow but then rapid, as in the APS–TEMED-initiated reactions. As shown below, replacing TEMED with SPS as the accelerator significantly affects the degree of inhomogeneity in both PAAm and PDMA hydrogels. Using the APS–SPS initiator system, we were able to produce relatively homogeneous hydrogels over a wide range of crosslink densities.

EXPERIMENTAL

Materials

Acrylamide (AAm, Merck, Darmstadt, Germany), *N,N*-dimethylacrylamide (DMA, Fluka, Buchs, Switzerland), *N,N′*-methylenebisacrylamide (BAAm, Merck), ammonium persulfate (APS, Merck), sodium metabisulfite (SPS), and *N,N,N′,N′*-tetramethylethylenediamine (TEMED) were used as received. Distilled and deionized water (HPLC grade) was used throughout this study. The stock solutions in water were prepared using the following concentrations: AAm (9.62 g/50 mL), BAAm (0.4 g/50 mL), APS (0.1143 g/20 mL), and SPS (0.0951 g/20 mL).

Crosslinking polymerization procedure

Free-radical crosslinking copolymerization reactions of AAm/BAAm and DMA/BAAm comonomer pairs were carried out in aqueous solutions at 21°C at a total monomer concentration, C_0, of 5.0 w/v%. To initiate the polymerization, the redox pairs consisting of APS (3.51 mM) – TEMED (24.9 mM) as well as APS–SPS (both 1.50 mM) were used in our experiments. These optimum concentrations of the redox pairs, providing gelation times in the reaction systems of less than 1 h, were determined by the preliminary experiments. Several sets of experiments were carried out. The gel synthesis parameters that varied were the type of the initiator system and the crosslinker ratio, denoted by X (the mole ratio of BAAm to AAm or DMA). The reactions were carried out in glass tubes, in light-scattering vials, as well as in glass dilatometers.

To illustrate the synthetic procedure in glass tubes, we give details for the preparation of a PAAm gel at $X = 1/50$ and using the APS–SPS redox pair: Stock solutions of APS (0.60 mL), AAm (2.50 mL), and BAAm (2.61 mL) were mixed in a 10-mL graduated flask. Then, SPS stock solution (0.6 mL) and water were added to give a total volume of 10 mL. The solution was then poured into several glass tubes of 4.5–5 mm internal diameters and about 100 mm long. The glass tubes were sealed and the polymerization was conducted at 21°C for a predetermined reaction time. The gel samples thus obtained were subjected to the mechanical tests, as described below.

To monitor the scattered light intensity as a function of time, the crosslinking polymerizations were also carried out in the light-scattering vials. All glassware was kept dustfree by rinsing in hot acetone prior to use. The preparation of the reaction solutions and the polymerization procedure were similar, as described above. The reaction solutions were filtered through membrane filters (pore size = 0.2 μm) directly into the vials. This process was carried out in a dustfree glovebox. All the solutions subjected to light-scattering measurements were clear and appeared homogeneous to the eye. The time evaluation of the scattered light intensity was measured at 21°C using a commercial multi-angle light-scattering DAWN EOS (Wyatt Technologies, Santa Barbara, CA) equipped with a vertically polarized 30 mW gallium-arsenide laser operating at $\lambda = 690$ nm and 18 simultaneously detected scattering angles. The light-scattering system was calibrated against a toluene standard (Rayleigh ratio at 690 nm = 9.7801×10^{-6} cm^{-1}, DAWN EOS software). The scattered light intensities were recorded from a scattering angle $\theta = 90°$ as a function of the reaction time.

For gel samples after 1 day of preparation, the scattered light intensities were recorded from angles $\theta = 14.5°$ to 163.3°, which correspond to the scattering vector q range $3.1 \times 10^{-4} - 2.4 \times 10^{-3}$ A$^{\circ\,-1}$, where $q = (4\pi n/\lambda)\sin(\theta/2)$, n is the refractive index of the medium. To obtain the ensemble averaged light-scattering intensity of gels, eight cycles of measurements with a small rotation of the vial between each cycle were averaged. For the calculation of excess scattering from gels, all the crosslinking polymerizations were repeated under the same experimental conditions except that the crosslinker BAAm was not used.[13]

Dilatometry

Linear polymerizations of AAm and DMA were also carried out in dilatometers consisting of a blown glass bulb, ~ 25 mL in volume connected to a 30-cm length of 1.5 mm precision-bore capillary tubing with a ground-glass joint.[20] The radius of the capillary was calibrated using mercury. During the reactions the meniscus of the liquid column in the capillary was read with a millimetric paper to 0.2 mm. The reproducibility of the kinetic data was checked by repeating the experiments as well as by the gravimetric measurement of the monomer conversions at certain time intervals.[21–23] The deviation in the time vs. conversion data was always less than 3%. The conversion of monomers x at the reaction time t was calculated as:

$$x = \frac{\pi r^2}{V_0 \alpha_C} \Delta h \tag{1}$$

where r is the radius of the capillary, V_0 is the volume of monomers in the dilatometer, α_C is the contraction factor, and Δh is the height change of the liquid column in the capillary between time zero and time t, respectively. The contraction factors α_C for AAm and DMA polymerizations were found by gravimetric determination of the monomer conversions to be 0.330 and 0.245, respectively.

Characterization of linear polymers

Linear PAAm and PDMA prepared in the presence of APS–TEMED as well as APS–SPS redox initiator systems were isolated after a reaction time of 1 h by precipitation of the diluted reaction solutions in acetone. They were then dried in vacuum at room temperature to constant weight. Solutions of the polymers with concentrations in the range of $4 \times 10^{-4} - 1 \times 10^{-3}$ g/mL in water were prepared from the dry polymer samples. The solutions were filtered as described above and light-scattering measurements were carried out using the DAWN EOS at $\lambda = 690$ nm and at scattering angles between 34° and 132°. The refractive index increment dn/dc was determined using the same polymer solutions using DAWN Optilap DSP at 690 nm. The dn/dc values of the polymers in water were found to be 0.163 and 0.166 mL/g for PAAm and PDMA, respectively. The weight-average molecular weight, $\overline{M}_w$, and the radius of gyration, $\langle R_g^2 \rangle^{1/2}$, of the polymers obtained from the Zimm plots are collected respectively in the third and fourth columns of Table I. From the molecular weight and the radius of the polymer chains, the critical overlap concentration, c^*, was calculated using the equation:[24]

$$c^* = \frac{\overline{M}_w / N_A}{\left(\frac{4}{3}\pi \left\langle R_g^2 \right\rangle^{3/2}\right)} 10^2 \tag{2}$$

where N_A is Avogadro's number. The calculated values of c^* in w/v% are shown in the fifth column of Table I.

Gel points

Gel point measurements were carried out in light-scattering vials containing the reaction solution and a PTFE-covered steel sphere.[22,23] The record of the reaction time was started after crossing the induction period, at which an abrupt increase in the scattered light intensity was observed (Fig. 2). The midpoint between the last time at which the sphere moved magnetically and that at which it stopped moving was taken as the gel point.

Swelling measurements

The hydrogels in the form of rods 4 mm in diameter were cut into samples of about 10 mm length. Then each sample was placed in an excess of water at 21°C. In order to reach swelling equilibrium, the hydrogels were immersed in water for at least 2 weeks, replacing the water every other day. The swelling equilibrium was tested by measuring the diameter of the gel samples. The normalized volume of the equilibrium swollen hydrogels, V_{rel} (volume of equilibrium swollen gel/volume of the gel just after preparation), was determined by measuring the diameter of the hydrogel samples by a calibrated digital compass (Mitutoyo

TABLE I
Characteristics of the Linear PAAm and PDMA Prepared Using APS–TEMED and APS–SPS Redox Pairs

Polymer	Initiator	$10^{-5}\,\overline{M}_w$ (g/mol)	$\left\langle R_g^2 \right\rangle^{1/2}$ (nm)	c^* (g/100 mL)	t^* (min)	t at $I_{s,max}$ (min)
PAAm	APS–TEMED	6.9 (0.3)	42 (3)	0.37 (0.08)	0.8 (0.1)	0.6 (0.1)
	APS–SPS	2.8 (0.1)	32 (4)	0.34 (0.10)	7.5 (0.3)	9 (0.5)
PDMA	APS–TEMED	14 (1)	62 (2)	0.23 (0.02)	0.7 (0.05)	0.4 (0.2)
	APS–SPS	1.9 (0.03)	17 (3)	1.6 (0.6)	12 (1)	12.5 (1)

$\overline{M}_w$ and $\left\langle R_g^2 \right\rangle^{1/2}$ are the weight average molecular weight and radius of gyration of the polymers, respectively, c^* is the overlap concentration calculated using Eq. (2). t^* is the critical reaction time at the chain overlap. The data in the last column show the reaction times t at the peak maximum in the scattering curves. The numbers in parentheses are the standard deviations.

[Tokyo, Japan] Digimatic Caliper, Series 500, resolution: 0.01 mm). V_{rel} was calculated as $V_{rel} = (D/D_0)^3$, where D and D_0 are the diameters of hydrogels after equilibrium swelling in water and after synthesis, respectively.

Mechanical measurements

All the mechanical measurements were conducted in a thermostated room of 21 ± 0.5°C. Uniaxial compression measurements were performed on gel samples prepared in glass tubes at the state of gel preparation. For this purpose, the gels in the form of rods of 4–5 mm in diameter were cut into samples of about 10 mm length. Then each cylindrical gel sample was placed on a digital balance.[25] A load was transmitted vertically to the gel through a rod fitted with a PTFE endplate. The force acting on the gel was calculated from the reading of the balance m as $F = m\,g$, where g is the gravitational acceleration. The resulting deformation, $\Delta l = l_0 - l$, where l_0 and l are the initial undeformed and deformed lengths, respectively, was measured using a digital comparator (IDC type Digimatic Indicator 543-262, Mitutoyo), which was sensitive to displacements of 10^{-3} mm. The force and the resulting deformation were recorded after 20 s of relaxation. The measurements were conducted up to about 20% compression. The deformation ratio, α (deformed length / initial length), was calculated as $\alpha = 1 - \Delta l/l_0$. The corresponding stress, f, was calculated as $f = F/A$, where A is the cross-sectional area of the specimen, $A = \pi\, r_0^2$, where r_0 is its initial radius. The elastic modulus, G_o, of gels just after their preparation was determined from the slope of linear dependence $f = G_0\,(\alpha - \alpha^{-2})$.

RESULTS AND DISCUSSION

Linear polymerization

We first conducted the polymerization reactions in the absence of the crosslinker BAAm. The initial monomer concentration was kept at 5.0 w/v%. The reactions were followed by both dilatometry and light scattering. The results of the dilatometric measurements are shown in Figure 1, where the fractional monomer conversion x is plotted against the reaction time in AAm (circles) and in DMA (triangles) polymerizations. The filled and open symbols are the data points obtained using APS–TEMED and APS–SPS initiator systems, respectively. The inset in Figure 1 shows the initial period of the reactions. It is seen that the polymerization of both AAm and DMA monomers in the presence of the APS–SPS initiator system is initially slowed to about 5–7 min. The monomer conversion attained after this slow period is about 2–4%. Thereafter, the polymerization occurs very rapidly, as in the presence of the APS–TEMED redox pair, and a complete monomer conversion was obtained after a reaction time of 90 min. As mentioned in the Introduction, the existence of various consecutive reactions for the radical generation by the APS–SPS redox pair seems to be responsible for this behavior. In Figure 2 the scattered light intensity, I_s, recorded at $\theta = 90°$, is shown as a function of the reaction time in AAm and DMA polymerizations using the APS–TEMED and APS–SPS redox pairs. For comparison, conversion curves are also shown in the figure. As expected, no intensity rise was observed during the induction period of the reactions. Therefore, the reaction time is defined as the total time elapsed minus the time needed for the induction period. The start of the polymerization is accompanied with a rapid increase in I_s, which reaches a maximum after a certain reaction time. Compared to TEMED, SPS as an accelerator produces only a smooth maximum in the scattered light intensity I_s at much longer reaction times. After passing the maximum intensity, I_s gradually decreases with the reaction time or monomer conversion, and finally attains a plateau value after about 15 min.

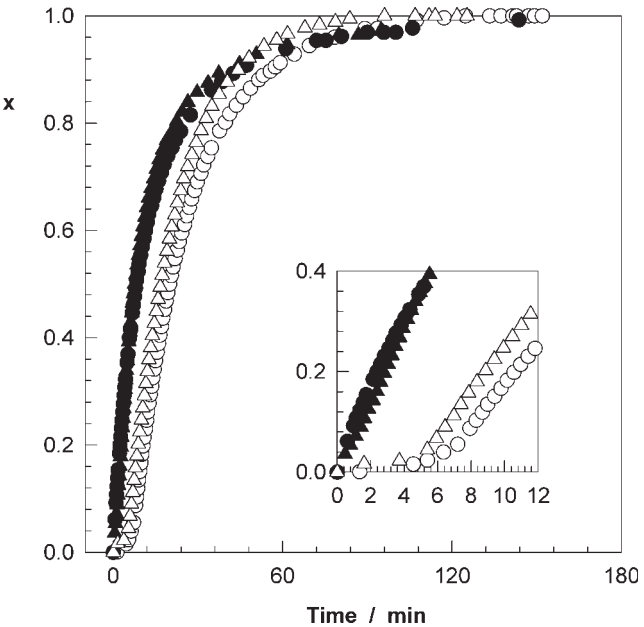

Figure 1 The fractional monomer conversion x plotted against the reaction time in linear AAm (circles) and DMA (triangles) polymerizations. Initial monomer concentration: $C_0 = 5.0\%$. Initiator system: APS–TEMED (filled symbols), APS–SPS (open symbols). The inset shows the initial period of the reactions.

The shape of the scattering curves shown in Figure 2 can be explained as follows:[15] The polymer chains formed during the reactions are initially in a highly dilute solution so that the polymer concentration, c, is below the so-called overlap threshold, c^*, where the chains start to overlap. As a result, the single coils

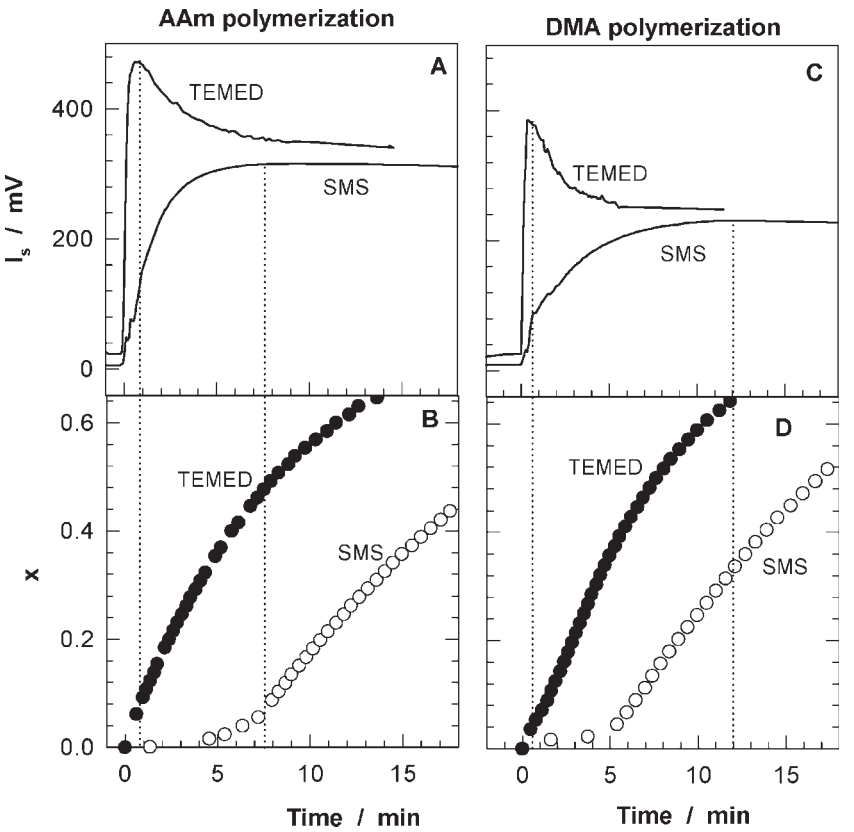

Figure 2 The scattered light intensity I_s recorded at $\theta = 90^\circ$ (A,C) and the monomer conversion x (B,D) shown as a function of the reaction time in linear AAm (left) and DMA polymerizations (right). $C_0 = 5.0\%$. The dotted vertical lines indicate the critical reaction times t^* at the chain overlap. APS was used as the initiator together with the accelerator indicated in the figures.

scatter light intensively and an abrupt intensity rise is observed with the onset of reactions. As the reactions proceed, the polymer concentration c increases and when c becomes larger than c^*, a semidilute polymer solution forms in the reaction system, where the chains overlap and the average mesh size is the characteristic size of the entangled chains. In this regime, only the mesh size of the polymer solution is detectable by light scattering and not the size of the individual polymer coils. Since the mesh size is much smaller than the size of molecules, the scattered light intensity decreases with the reaction time. Accordingly, the maximum in the scattering curves can be interpreted as the point at which the polymer concentration in the reaction system attains the critical overlap concentration c^*. In order to check this point, the critical reaction times, t^*, for the onset of chain overlap were calculated using the c^* concentrations listed in Table I together with the time conversion curves. The calculated values of t^* together with the reaction times t at the peak maxima are listed in Table I. The vertical dotted lines in Figure 2 also represent t^* values on the time axes. For all the reaction systems studied, it is shown that the maximum in the scattering curves coincides with c^* of the polymerization systems. These results also demonstrate that the combination of dilatometric and real-time light-scattering techniques provides an experimental tool for the determination of the critical overlap concentration in linear polymerization systems.

Table I also shows that the average size of PDMA coils formed using APS–SPS is much smaller compared to those formed using the APS–TEMED redox pair. As a consequence, PDMA chains in APS–SPS-initiated reactions start to overlap at a longer reaction time (12 vs. 0.7 min), so that the maximum of the scattering curve shifts toward a later reaction time. In AAm polymerization, however, the decrease in the coil size is not as significant as in the DMA polymerization, so that c^* does not change much when the initiator system was changed (Table I). However, in this case, since the initial rate of APS–SPS initiated polymerization is slow, t^* also shifts toward a longer reaction time.

Crosslinking polymerizations

Crosslinking polymerization reactions were carried out under the same reaction conditions as the corresponding linear polymerizations. Figure 3(A,B) shows

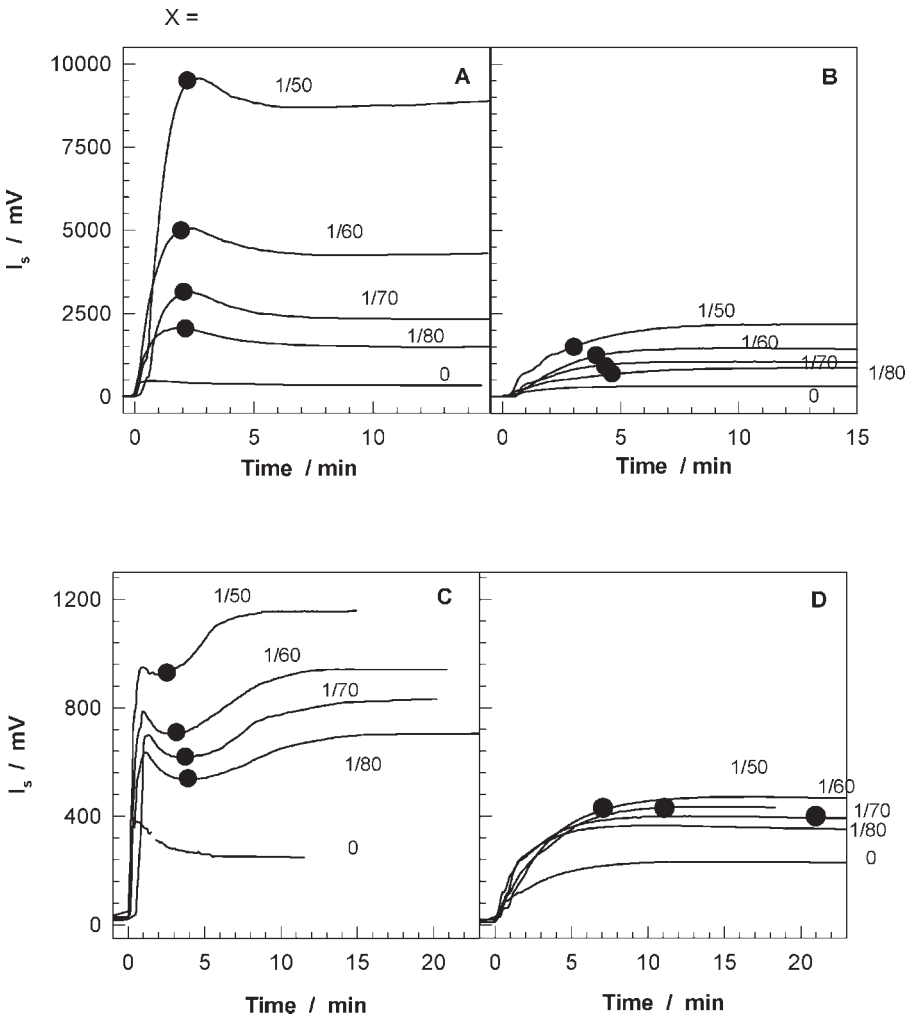

Figure 3 The scattered light intensity I_s at $\theta = 90^\circ$ vs. reaction time plots for crosslinking AAm (A,B) and DMA polymerizations (C,D). Initiator system: APS–TEMED (A,C), and APS–SPS (B,D). $C_0 = 5.0\%$. The crosslinker ratios X are indicated in the figures. The filled symbols illustrate the gel points in terms of the reaction times.

the scattering intensity I_s vs. reaction time plots for crosslinking AAm polymerizations initiated by the APS–TEMED and APS–SPS redox pairs, respectively. Here we varied the crosslinker ratio X between 1/80 and 1/50, keeping the total monomer concentration at 5.0 w/v%. The data obtained in linear polymerizations ($X = 0$) are also shown in the figure. The filled circles illustrate the gel points in terms of the reaction times. The shape of I_s vs. time plots is the same with and without crosslinker. The larger X is the stronger is the increase of I_s, which is obviously due to crosslinking reactions leading to the formation of larger molecules. However, if SPS is used as an accelerator instead of TEMED, no significant intensity rise was observed during the crosslinking AAm polymerization. A comparison of the gel points also shows that the gel formation is retarded by replacing TEMED with SPS accelerator. Figure 3(C,D) shows I_s vs. reaction time plots for crosslinking DMA polymerizations using APS–TEMED and APS–SPS redox pairs, respectively. The scattering intensity profile during the formation of PDMA gels by APS–TEMED exhibits both a maximum and a minimum, corresponding to the overlap threshold and the gel point, respectively [Fig. 3(C)]. This difference in the time-course between DMA and AAm gel formation systems is due to the late onset of gelation in the DMA system with respect to the critical overlap concentration. This finding is in accord with our previous observations.[15] Similar to the AAm system, the larger the X, the stronger the scattered intensity I_s along the DMA polymerization. Moreover, the intensity increase with the crosslinker ratio is also reduced if SMS is used as the accelerator. Another distinction between the APS–TEMED and APS–SPS-initiated reactions appeared in the growth of the gel molecule. For the APS–SPS system, the gel point was a point at which a soft gel in the lower part of the reactor starts to appear. It required a few hours until the gel occupied the entire polymerization system. However, the formation and growth of gel in

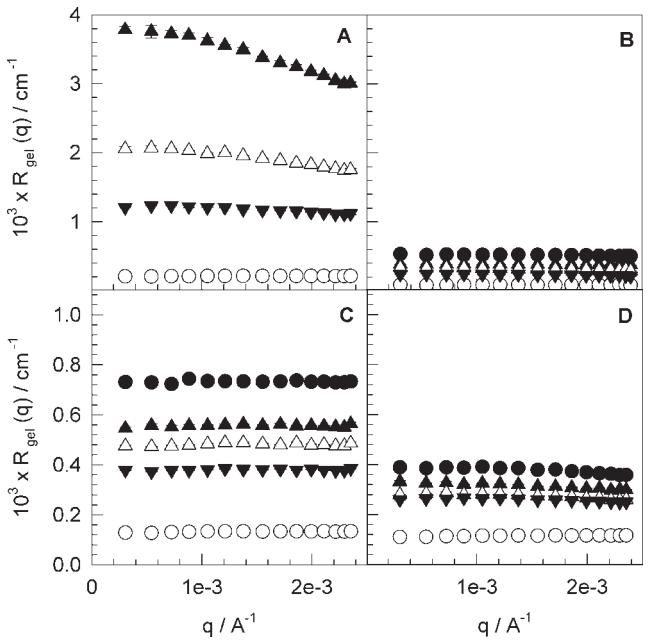

Figure 4 Rayleigh ratio R_{gel}(q) vs. scattering vector q plots for PAAm (A,B) and PDMA gels (C,D). $C_0 = 5.0\%$. Reaction time = 24 h. Initiator system: APS–TEMED (A,C), and APS–SPS (B,D). $X = 1/50$ (●), 1/60 (▲), 1/70 (△), 1/80 (▼), and 0 (○).

APS–TEMED system took place within 1 min. This distinction may be attributed to the lower efficiency of crosslinking in APS–SPS-initiated reactions, as described below.

The results in Figure 3 clearly show that the scattered light intensity during gelation of both AAm and DMA monomers is significantly reduced when the APS–SPS initiator system is used for the radical generation. To generalize this finding, we investigated the properties of completely formed PAAm and PDMA hydrogels under various crosslinker ratios. The reaction time was set to 24 h. Figure 4 shows the Rayleigh ratio, $R_{gel}(q)$, vs. the scattering vector q plots for PAAm and PDMA gels formed at various crosslinker ratios. When TEMED is used as an accelerator the scattering intensity from both PAAm and PDMA gels significantly increases with the crosslinker ratio X. At $X = 1/50$, PAAm gels were opaque, indicating that these gels have heterogeneities in a spatial scale of submicrometer to micrometer. However, when SPS is used as an accelerator, the intensity rise with the crosslinker ratio is much smaller [Fig. 4(B,D)]. Figure 4 also shows that the light-scattering intensity does not change much with the scattering vector q. This is expected, since we are probing length scales large compared with those typical for polymer gels. Therefore, in the following we focus on the scattering intensities measured at a fixed scattering angle, $\theta = 90^\circ$. The excess scattering over the scattering from polymer solution $R_{ex,q}$ was calculated as $R_{ex,q} = R_{gel,q} - R_{sol,q}$, where $R_{gel,q}$ and $R_{sol,q}$ are the Rayleigh ratios for gel and polymer solution at a fixed scattering vector q, respectively. Figure 5 shows the excess scattering $R_{ex,q}$ of PAAm (circles) and PDMA gels (triangles) plotted as a function of the inverse crosslinker ratio $1/X$ (mole monomer/mole crosslinker). Regardless of the crosslinker ratio, the excess scattering intensities from gels formed using SPS are much smaller that those formed using the TEMED accelerator. The decrease in $R_{ex,q}$ is particularly significant in PAAm gels. Since the thermal concentration fluctuations in gels are eliminated in $R_{ex,q}$, excess scattering is a measure of the degree of spatial inhomogeneities. Thus, the results demonstrate that the extent of the inhomogeneities in both PAAm and PDMA gels is strongly reduced when a APS–SPS redox pair is used in the gel preparation.

To interpret the light-scattering results from gels, several Lorentzian and Gaussian scattering functions have been proposed empirically.[3,4] For example, the excess scattering $R_{ex}(q)$ was given by the Debye–Bueche (DB) function as:

$$R_{ex}(q) = \frac{4\pi\ K\ \xi^3 \langle \eta^2 \rangle}{(1 + q^2\ \xi^2)^2} \tag{3}$$

where K is the optical constant, $K = 8\pi^2\ n^2\ \lambda^{-4}$, ξ is the correlation length of the scatterers, and $\langle \eta^2 \rangle$ is the mean square fluctuation of the refractive index. Note that the correlation length ξ of DB theory is a characteristic length scale in the gel and, it is a measure of

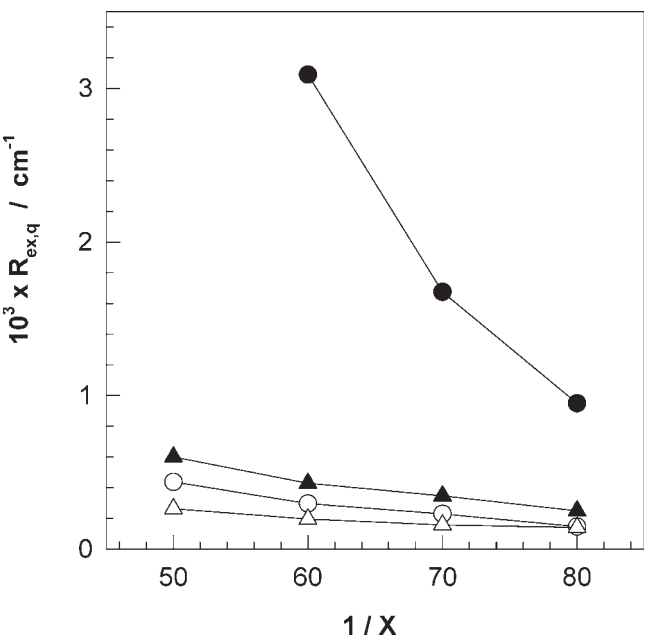

Figure 5 The excess scattering $R_{ex,q}$ measured at $\theta = 90^\circ$ shown as a function of $1/X$ for PAAm (circles) and PDMA gels (triangles). $C_0 = 5.0\%$. Reaction time = 24 h. Initiator system: APS–TEMED (filled symbols), and APS–SPS (open symbols).

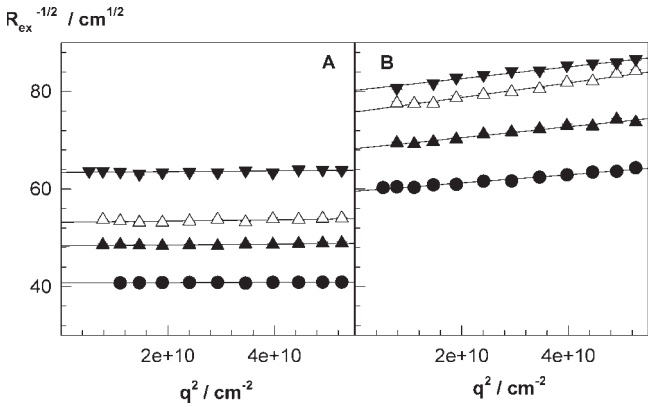

Figure 6 Debye–Bueche plots for PDMA gels prepared using APS–TEMED (A) and APS–SPS (B) redox pairs. X = 1/50 (●), 1/60 (▲), 1/70 (△), and 1/80 (▼).

the spatial extent of the fluctuations. According to Eq. (3), the slope and the intercept of $R_{ex}\,(q)^{-1/2}$ vs. q^2 plot (DB plot) give ξ and $\langle\eta^2\rangle$ of a gel sample. In Figure 6 the data points shown in Figure 4 for PDMA gels are replotted in the form of DB plots. It is seen that straight lines are obtained in this analysis, indicating that the DB function works well. The calculated values of ξ and $\langle\eta^2\rangle$ from DB analysis are shown in Figure 7 for PDMA gels plotted as a function of $1/X$. The correlation length of the scatterers ξ, i.e., the extension of the inhomogeneities in gels, is 10^1 nm, while the extent of the concentration fluctuations $\langle\eta^2\rangle$ is in the range 10^{-6}–10^{-3}. Further, ξ increases while $\langle\eta^2\rangle$ decreases if SPS is used as the accelerator in the gel preparation. Similar results as those in Figures 6 and 7 were also obtained for the PAAm gels.

Figure 8(A,B) shows the elastic modulus G_0 and the equilibrium swelling ratio V_{rel} of PAAm (circles) and PDMA gels (triangles) plotted against the inverse crosslinker ratio $1/X$. Filled and open symbols represent data from gels obtained using the APS–TEMED and APS–SPS redox pairs, respectively. As expected, G_0 increases while V_{rel} decreases with the crosslinker concentration. Moreover, gels formed using APS–TEMED exhibit larger elastic moduli and a smaller degree of swelling in water compared to those formed using the APS–SPS initiator system. Assuming that all BAAm molecules used in the gel synthesis participate in forming effective crosslinks, theoretical elastic modulus G_{theo} of the hydrogels can be calculated as:[26,27]

$$G_{theo} = A\frac{2\rho X}{M_r}RTv_2^0 \qquad (4)$$

where the front factor A equals 1 for an affine network and 1-2/ϕ for a phantom network, ϕ is the functionality of the crosslinks, ρ is the polymer density (1.35 and 1.21 g/mL for PAAm and PDMA gels, respectively), M_r is the molecular weight of repeat unit (71 and 99 g/mol for AAm and DMA, respectively), v_2^0 is the polymer concentration just after the gel preparation, and R and T have their usual meanings. Assuming phantom network behavior (ϕ = 4), G_{theo} of the hydrogels calculated using Eq. (4) are also shown in Figure 8(A) as dotted curves. It is seen that G_{theo} is much higher than G_0 of the hydrogels. The crosslinking efficiency of BAAm $\varepsilon_{xl} = G_0/G_{theo}$ that is the fraction of BAAm forming effective crosslinks is shown in the Figure 8(C) as a function of $1/X$. When TEMED is used as an accelerator, ε_{xl} is in the range 0.10–0.15. This value is in good agreement with that found from the equilibrium swelling measurements of gels,[28] as well as from the determination of the pendant vinyl group content of pre-gel polymers.[22] The low efficiency of crosslinking ε_{xl} is mainly due to the cyclization and multiple crosslinking reactions during gelation, leading to the formation of elastically ineffective loops as well as clusters of crosslinks in the final network. However, if SPS is used as an accelerator, ε_{xl} further reduces to 10^{-2}–10^{-3}, indicating that only 0.1 to 1% of BAAm used in the hydrogel preparation form effective crosslinks in the final hydrogels. Figure 8(C) also shows that the decrease in the crosslinking efficiency due to the use of SPS is particularly significant in the DMA polymerization. This very low efficiency of crosslinking in APS–SPS system is probably due to the formation of low molecular weight polymers (Table I). Thus, as the primary molecules become shorter, the number of terminal chains, which make no contribution to the network elasticity, increases, so that the crosslinking efficiency decreases.

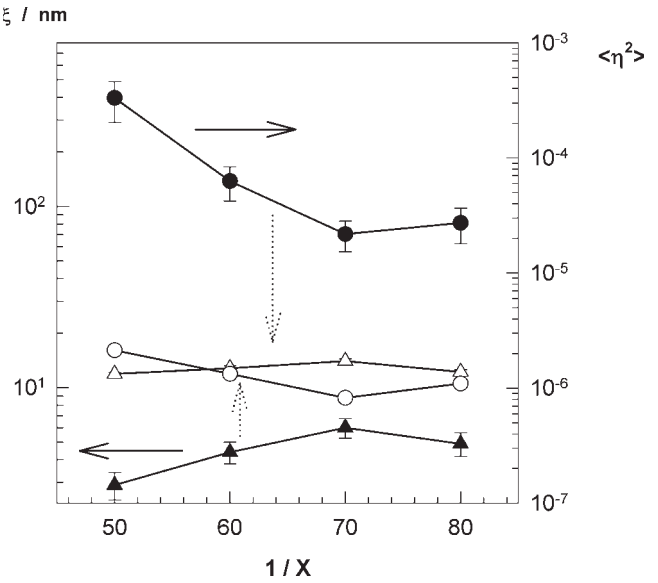

Figure 7 The correlation length ξ (triangles) and the mean square fluctuation of the refractive index $\langle\eta^2\rangle$ (circles) in PDMA gels shown as a function of the inverse crosslinker ratio $1/X$. C_0 = 5.0%. Reaction time = 24 h. Initiator system: APS–TEMED (filled symbols), and APS–SPS (open symbols).

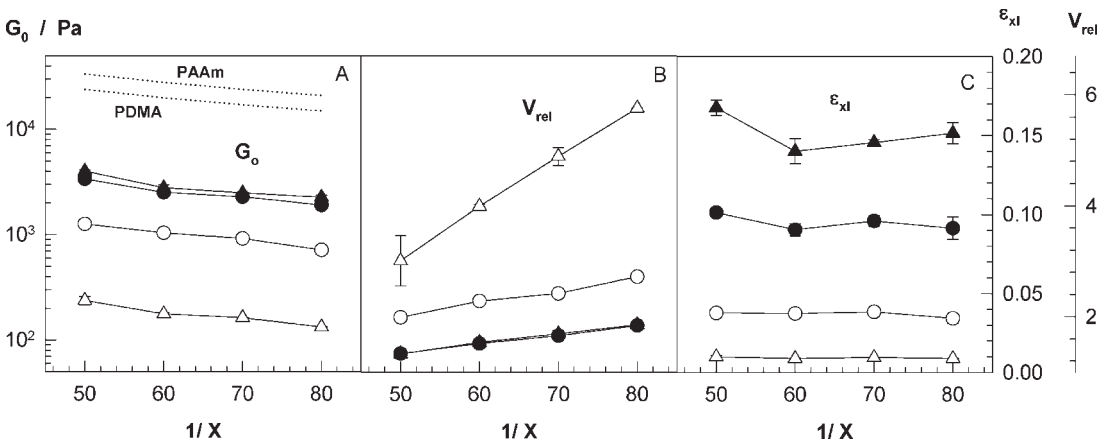

Figure 8 The elastic modulus of gels after preparation G_0 (A), the relative swelling ratio of the equilibrium swollen gels in water V_{rel} (B) and the crosslinking efficiency of BAAm ε_{xl} during the gel preparation shown as a function of $1/X$ for PAAm (circles) and PDMA gels (triangles). $C_0 = 5.0\%$. Reaction time = 24 h. Initiator system: APS–TEMED (filled symbols) and APS–SPS (open symbols). The theoretical elastic modulus G_{theo} vs. $1/X$ plot is shown by the dotted curves.

The following physical picture explains the results of our observations. As pointed out in the Introduction, cyclization and multiple crosslinking reactions are the main features of the gel formation processes of both PAAm and PDMA gels.[1,2,21] As illustrated schematically in Figure 9, cycles are formed when the macroradical attacks the pendant vinyl groups in the same kinetic chain, while multiple crosslinks are formed if the radical attacks double bonds pendant on other chains already chemically connected with the growing radical. As seen in Figure 9, the growing radical, shown by the dashed curve, first attacks the pendant vinyl group denoted by A. This is a typical crosslinking reaction and leads to the formation of an effective crosslink at point A. However, after this reaction the local concentration of the pendant vinyl groups around the radical rapidly increases so that the growing radical can further react with the pendant vinyl groups denoted by B, C, and D. These reactions lead to the formation of multiple crosslinks at B, C, and D. Thus, although cycles are intramolecular links, multiple crosslinks are elastically effective links in a small region of space. The regions where the multiple crosslinks form have a higher crosslink density than do others, so that they will not swell as much as the other regions. As a result, the inhomogeneous distribution of effective crosslinks and the resulting concentration fluctuations $\langle \eta^2 \rangle$ in gels are a result of multiple

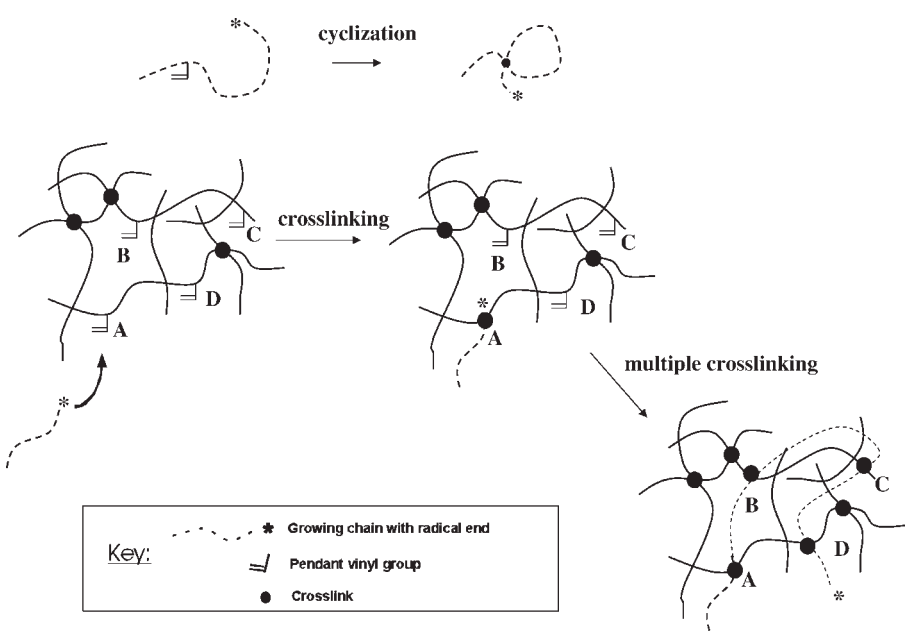

Figure 9 Schematic representation of cyclization and multiple crosslinking reactions in free-radical crosslinking copolymerization.

crosslinking reactions. As seen in Table I, APS–SPS initiator system produces lower molecular weight polymers compared to the APS–TEMED system. Since decreasing the chain length of polymers necessarily reduces the extent of the multiple crosslinking reactions,[29] a more homogeneous distribution of the crosslink points along the gel sample was obtained using the APS–SPS initiator system. Moreover, the shift of the gel point to longer reaction times in APS–SPS-initiated crosslinking reactions also contributes to the homogeneity of the resulting gels. This is due to the fact that the late gelation in the crosslinking polymerization using the APS–SPS initiator system produces a gel that is much more concentrated than that formed using the APS–TEMED system.[15] Since increasing polymer concentration reduces the concentration difference between dense and loose regions of the gel,[13] the gels formed using the APS–SPS initiator system exhibit a lesser degree of inhomogeneity. As the degree of inhomogeneity decreases, the highly crosslinked region of gel absorbs more solvent (water) after the preparation state. As a consequence, their size, represented by ξ, increases, while the extent of the concentration fluctuations $\langle \eta^2 \rangle$ decreases (Fig. 7).

CONCLUSIONS

PAAm and PDMA hydrogels were prepared by free-radical crosslinking copolymerization of the monomers AAm and DMA, respectively, with BAAm as a crosslinker. Two different redox-initiator systems, APS–TEMED and APS–SPS, were used to initiate the gelation reactions. The reactions were monitored by real-time light-scattering measurements as well as by dilatometry. The results showed that the combination of dilatometric and real-time light-scattering techniques provides an experimental tool for the determination of the critical overlap concentration in the polymerization systems. Compared to the APS–TEMED redox pair, no significant scattered light intensity rise was observed during the crosslinking polymerization reactions initiated by the APS–SPS system. It has been shown that both PAAm and PDMA gels are much more homogeneous when the APS–SPS redox pair was used as the initiator. The results are explained by the formation of shorter primary chains as well as the delay of the gel point in the APS–SPS-initiated gel formation reactions.

References

1. Funke, W.; Okay, O.; Joos-Muller, B. Adv Polym Sci 1998, 136, 139.
2. Okay, O. Prog Polym Sci 2000, 25, 711.
3. Shibayama, M. Macromol Chem Phys 1998, 199, 1.
4. Bastide, J.; Candau, S. J. In Physical Properties of Polymeric Gels; Cohen Addad, J. P. Ed.; John Wiley & Sons: New York. 1996; p 143.
5. Mallam, S.; Horkay, F.; Hecht, A. M.; Geissler, E. Macromolecules 1989, 22, 3356.
6. Ikkai, F.; Shibayama, M. Phys Rev E 1997, 56, R51.
7. Cohen, Y.; Ramon, O.; Kopelman, I. J.; Mizraki, S. J Polym Sci Polym Phys Ed 1992, 30, 1055.
8. Schosseler, F.; Skouri, R.; Munch, J. P.; Candau, S. J. J Phys II 1994, 4, 1221.
9. Shibayama, M.; Tanaka, T.; Han, C. C. J Chem Phys 1992, 97, 6842.
10. Horkay, F.; McKenna, G. B.; Deschamps, P.; Geissler, E. Macromolecules 2000, 33, 5215.
11. Yazici, I.; Okay, O. Polymer 2005, 46, 2595.
12. Kizilay, M. Y.; Okay, O. Polymer 2003, 44, 5239.
13. Kizilay, M. Y.; Okay, O. Macromolecules 2003, 36, 6856.
14. Kizilay, M. Y.; Okay, O. Polymer 2004, 45, 2567.
15. Orakdogen, N.; Kizilay, M. Y.; Okay, O. Polymer 2005, 46, 11407.
16. Feng, X. D.; Guo, X. Q.; Qiu, K. Y. Makromol Chem 1988, 189, 77.
17. Ebdon, J. R.; Hunckerby, T. N.; Hunter, T. C. Polymer 1994, 35, 251.
18. Bokias, G.; Durand, A.; Hourdet, D. Makromol Chem Phys 1994, 199, 1387.
19. Mukherjee, A. R.; Ghosh, P.; Chadha, S. C.; Palit, S. R. Makromol Chem 1966, 97, 202.
20. Okay, O.; Naghash, H. J.; Capek, I. Polymer 1995, 36, 2413.
21. Okay, O.; Kurz, M.; Lutz, K.; Funke, W. Macromolecules 1995, 28, 2728.
22. Naghash, H. J.; Okay, O. J Appl Polym Sci 1996, 60, 971.
23. Durmaz, S.; Okay, O. Polymer 2000, 41, 3693.
24. De Gennes, P. G. Scaling Concepts in Polymer Physics. Cornell University Press: Ithaca, NY, 1979.
25. Sayil, C.; Okay, O. Polymer 2001, 42, 7639.
26. Flory, P. J. Principles of Polymer Chemistry. Cornell University Press: Ithaca, NY, 1953.
27. Treloar, L. R. G. The Physics of Rubber Elasticity. University Press: Oxford, 1975
28. Okay, O.; Sariisik, S. B. Eur Polym J 2000, 36, 393.
29. Cerid, H.; Okay, O. Eur Polym J 2004, 40, 579.